



## EVREST Project Report: Fieldwork in Culatra Island

Project Funding: Fundação para a Ciência e a Tecnologia (FCT)

Scientific Domain: Marine Sciences and Earth Sciences - Estuarine Coastal and Littoral Systems

Project reference: PTDC/MAREST/1031/2014

<b>Report Title</b>	Fieldwork in Culatra Island
<b>Reporting Period</b>	May to June, 2017
<b>Delivery Date</b>	30/11/2017
<b>Related Task</b>	Task 1: Data collection and GIS integration
<b>Objective</b>	Mapping marsh topography, vegetation, sedimentation rates and sediment sampling
<b>Participants</b>	Ana Matias, Katerina Kombiadou, Rita Carrasco, Susana Costas, Margarida Ramires, Emily Robbins and Luisa Bom de Sousa

## TABLE OF CONTENTS

<b>Summary of Fieldwork .....</b>	<b>1</b>
<b>1 Equipment and Measurements.....</b>	<b>1</b>
1.1 Equipment and stations .....	1
1.2 Sediment core sectioning.....	5
<b>2 Measurement results .....</b>	<b>9</b>
2.1 Profiling .....	9
2.2 Surface Sediment Properties .....	11
2.3 Sediment Core analysis .....	13
2.3.1 Grain-size analysis of core C1 .....	13
2.3.2 Grain-size analysis of core C2 .....	15
2.3.3 Grain-size analysis of core C3 .....	17
<b>3. Identification of Intertidal and Marsh Vegetation.....</b>	<b>20</b>
<b>References.....</b>	<b>30</b>

## TABLE OF FIGURES

<b>Figure 1:</b> Location of the EVREST study site in Culatra (orange polygon). ....	1
<b>Figure 2:</b> Surface sediment (orange points) and sediment core sampling stations (green points) and GNSS transects (lines that correspond to measurements on 01/06 [blue], 02/06 [green] and 29/06 [purple]).....	3
<b>Figure 3:</b> Sediment facies from sediment core C3.....	6
<b>Figure 4:</b> Trajectories of three tracks, whose measurements are indicatively presented. The direction of each track is presented as dashed arrow, while for Track 3, characteristic positions along the trajectory are given in as numbers 3.1 to 3.5.....	9
<b>Figure 5:</b> Profile along Track 1 (location of track is given in figure 4).....	10
<b>Figure 6:</b> Profile along Track 2 (location of track is given in figure 4).....	10
<b>Figure 7:</b> Profile along Track 3 (location of track is given in figure 4 and positions of change in track direction are noted as points 3.1 to 3.5). ....	11
<b>Figure 8:</b> Distributions of sand, mud and gravel content and mean sediment diameter. The sampling stations' locations are noted with black dots.....	12
<b>Figure 9:</b> Organic content [%] and sediment sorting classification after Folk & Ward (1957). ....	13
<b>Figure 10:</b> Distribution with depth of: (b) percent gravel, sand and mud (with reference to the top x-axis) and mean sediment diameter (with reference to the bottom x-axis) and (c) of organic content from the granulometric analysis of Core C1. A photo of the entire core, in scale with the plots, is given in (a), while the sediment description (according to Folk & Ward, 1957) is also noted on the graph.....	14
<b>Figure 11:</b> Variability of mean sediment diameter with sediment sorting (left y-axis) and organic matter (right y-axis) in the sediment of core C1. ....	15
<b>Figure 12:</b> Particle size distribution for the upper three sediment layers of core C1. ....	15

<b>Figure 13:</b> Distribution with depth of: (b) percent gravel, sand and mud (with reference to the top x-axis) and mean sediment diameter (with reference to the bottom x-axis) and (c) of organic content from the granulometric analysis of Core C2. A photo of the entire core, in scale with the plots, is given in (a), while the sediment description (according to Folk & Ward, 1957) is also noted on the graph.....	16
<b>Figure 14:</b> Variability of mean sediment diameter with sediment sorting (left y-axis) and organic matter (right y-axis) of core C2. ....	17
<b>Figure 15:</b> Particle size distribution for the upper five sediment layers of core C2. ....	17
<b>Figure 16:</b> Distribution with depth of: (b) percent gravel, sand and mud (with reference to the top x-axis) and mean sediment diameter (with reference to the bottom x-axis) and (c) of organic content from the granulometric analysis of Core C3. A photo of the entire core, in scale with the plots, is given in (a), while the sediment description (according to Folk & Ward, 1957) is also noted on the graph.....	18
<b>Figure 17:</b> Variability of mean sediment diameter with sediment sorting (left y-axis) and organic matter (right y-axis) of core C3. ....	19
<b>Figure 18:</b> Particle size distribution for the upper five sediment layers of core C3. ....	19

## TABLE OF PHOTOS

<b>Photo 1:</b> The Trimble R6 GNSS system used in the survey .....	2
<b>Photo 2:</b> The metal corer used for core collection (a and b) and example of the core extracted in the tube (c).....	4
<b>Photo 3:</b> The core collection at C3 using a PVC tube.....	4
<b>Photo 4:</b> Photos from sediment core C3. ....	5
<b>Photo 5:</b> Zoom to the top of the sediment core C3, showing the organic matter deposition. ....	7
<b>Photo 6:</b> Photo from the first half of core C3, showing the moisture of organic matter and sand. ....	7
<b>Photo 7:</b> Photo from the second half of core C3, showing predominant medium sand. ....	8
<b>Photo 8:</b> Zoom to the bottom of the sediment core C3 showing organic matter presence. ....	8
<b>Photo 9:</b> Photos from stations 1, 2, 3 and 4 .....	21
<b>Photo 10:</b> Photos from stations 5, 6, 7 and 8 .....	22
<b>Photo 11:</b> Photos from stations 9, 14, 15 and 16 .....	23
<b>Photo 12:</b> Photos from stations 19, 20, 21 and 22 .....	24
<b>Photo 13:</b> Photos from station 24 and cores 1, 2 and 3 .....	25
<b>Photo 14:</b> <i>Spartina maritima</i> meadows, found at the low-upper part of the marsh (southern bay) .....	26
<b>Photo 15:</b> <i>Salicornia ramosissima</i> , found in the mid-upper part of the marsh (southern bay) .....	26
<b>Photo 16:</b> <i>Limoniastrum monopetalum</i> , found at the high-upper part of the marsh (southern bay) .....	27
<b>Photo 17:</b> Panorama of the entire study area (top), produced after stitching series of photographs taken from approximately the middle of the bay. Four characteristic points are noted in the panoramic view of the area and are related to a vertical photo of the bay (bottom), along with colour-gradated curves that denote the transition between points, to facilitate orientation. ....	28
<b>Photo 18:</b> Series of ‘panoramic’ photos for the southern part of the bay, where the vegetation species succession in the upper marsh can be noted. ....	29
<b>Photo 19:</b> Presence of <i>zostera marina</i> in the study area: a) at the edges of <i>zostera noltei</i> meadows and along the sandy channels (yellow box) and b) development of dense <i>zostera marina</i> meadows in the deeper parts of the northern bay (red box). ....	30

## TABLE OF TABLES

<b>Table 1:</b> Name, location (in the European Terrestrial Reference System 1989 [PT-TM06/ETRS89]) and elevation of the 35 surface sediment sampling stations and of the 3 core sampling stations (Core 1, Core 2 and Core 3 in table).....	2
--	---

## SUMMARY OF FIELDWORK

The present report refers on the measurements and sampling that took place during 2 field campaigns in the embayment of Culatra Island. The location of the embayment in Culatra, which is the EVREST study site for saltmarsh evolution, is given in figure 1.



**Figure 1:** Location of the EVREST study site in Culatra (orange polygon).

The measurements in the embayment concerned topographic mapping of the area, surficial sediment and sediment core sampling, as well as identification of mud and tidal flat vegetation.

## 1 EQUIPMENT AND MEASUREMENTS

### 1.1 Equipment and stations

The field mapping of elevation profiles in the Culatra embayment was carried out using a Trimble R6 Global Navigation Satellite System (GNSS) Receiver (Photo 1). The instrument (RTK-DGPS: Real-Time Kinematic Differential Global Positioning System) was used to collect position/elevation data (triads of x, y, z) along tracks in the bay, as well as to obtain the accurate position of sediment collection and vegetation identification stations. The location of the sediment sampling stations and the contiguous transects measured during the survey are presented in figure 2. Regarding the sediment sampling, a total of 35 surface samples (each weighing at least 200gr) were collected from the area and 3 sediment cores, using a manual metal corer with a 50cm core tube (Photo 2). Details on the location of the 35 surface sampling stations and of the 3 sediment cores collected are provided in table 1.

**Table 1:** Name, location (in the European Terrestrial Reference System 1989 [PT-TM06/ETRS89]) and elevation of the 35 surface sediment sampling stations and of the 3 core sampling stations (Core 1, Core 2 and Core 3 in table).

Station No	Easting [m]	Northing [m]	Z [m]	Station No	Easting [m]	Northing [m]	Z [m]
1	26442.98	-297040.56	-0.684	19	26456.79	-297269.03	0.496
2	26565.49	-297096.26	-0.219	20	26406.80	-297274.51	0.176
3	26562.04	-297149.63	0.439	21	26376.03	-297267.79	0.478
4	26535.61	-297127.28	0.195	22	26374.81	-297311.89	0.252
5	26520.42	-297114.36	0.109	23	26333.15	-297362.59	0.653
6	26452.11	-297096.60	-0.369	24	26408.38	-297264.09	0.127
7	26448.00	-297096.84	-0.418	25	26393.65	-297342.91	0.984
8	26442.49	-297051.03	-0.455	26	26383.23	-297371.79	1.054
9	26456.25	-297025.91	-0.496	27	26353.96	-297336.82	0.464
10	26418.42	-297018.40	-0.626	28	26316.82	-297374.34	0.865
11	26417.28	-297046.08	-0.621	29	26452.52	-297088.05	-0.229
12	26418.04	-297082.42	-0.489	30	26475.32	-297047.61	-0.607
13	26417.43	-297128.18	-0.274	31	26482.62	-297014.02	-0.880
14	26,390.71	-296,959.11	-0.1	32	26459.09	-296976.78	-0.588
14A	26410.17	-297198.6	0.012	33	26488.403	-296957.11	-0.508
15	26394.29	-297188.33	-0.088	34	26505.55	-296931.29	-0.482
16	26446.10	-297199.01	0.051	Core 1	26405.78	-297338.36	0.924
17	26463.90	-297204.37	0.005	Core 2	26433.22	-297268.50	0.384
18	26522.52	-297219.62	0.618	Core 3	26444.07	-297202.38	-0.215



**Photo 1:** The Trimble R6 GNNS system used in the survey

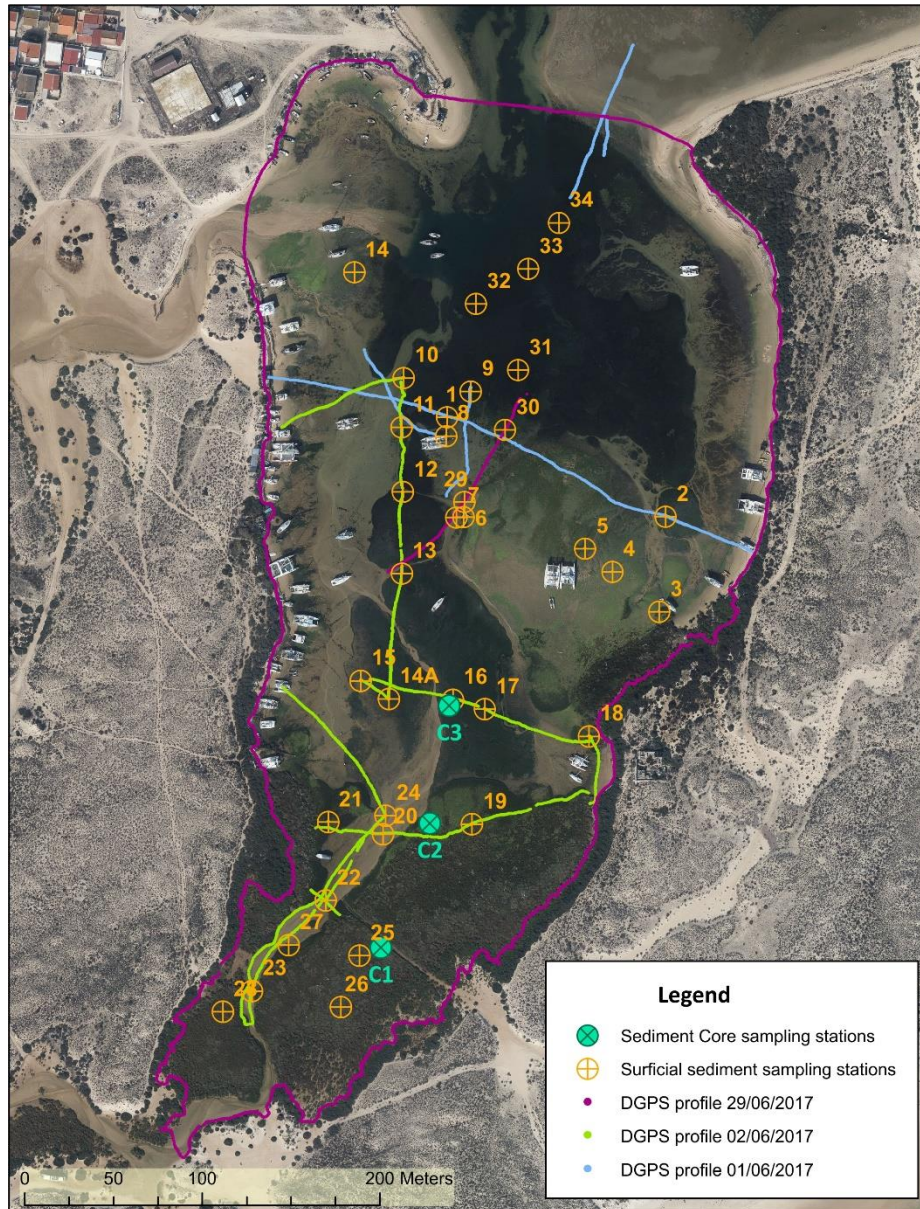


**Figure 2:** Surface sediment (orange points) and sediment core sampling stations (green points) and GNSS transects (lines that correspond to measurements on 01/06 [blue], 02/06 [green] and 29/06 [purple]).

Sediment cores from the high marsh (cores C1 and C2, see Figure 2 and table 1) were collected using a metal corer (Photo 2) and the sediment core from the low marsh (core C3, see Figure 2 and table 1) was collected using a PVC pipe of 70cm length and 4.5cm diameter. For the collection of the sample in C3, the tube was inserted in the soil (Photo 3), capped and removed with caution, so as to collect samples as undisturbed as possible.

The fieldwork was undertaken to characterise the local eco-geomorphological variety and to discuss the ecological development based on the local environmental settings. Collected samples and sediment cores were located using RTK-DGPS.



**Photo 2:** The metal corer used for core collection (a and b) and example of the core extracted in the tube (c).



**Photo 3:** The core collection at C3 using a PVC tube.

## 1.2 Sediment core sectioning

Cores C1 and C2 were sectioned on the field, right after collection of the core, sectioning every 2cm in the top layer and every 5cm for the bottom layer of the core. The samples were secured and labelled in plastic bags and were then analysed in the laboratory.

After collection, the sediment core C3 was carried to lab and was frozen until September 4<sup>th</sup>. The core was opened by September 6<sup>th</sup>. The sediment core presented about 57 cm of length and 4.5 cm of diameter (Photo 4). The core was split in several slices of 1 cm, using a spatula, from the top towards the base. Only 1/2 of the core was split, and the other 1/2 of the core was further used for grain size analysis. Plastic bags were used to store collected sediment samples. Bags are labelled with reference to the distance from top of the core: from 0-1cm, consecutive, until 56cm-57cm.



**Photo 4:** Photos from sediment core C3.

Figure 3 portrays the dominant sediment facies. The upper part of the core (1-12cm from top) it is the most organic rich, being composed of fragments of shells and plant material (Photo 5), deposited under lower energetic conditions. A second horizon is identified between the 12-22 cm from the top mostly composed of sand and very fine sediment (silty-sand). Between the 23-30 cm we observed the dominance of very fine sediment, silt and few shells (silt; Photo 6). In contrast, between the 31-42 cm from the top the core is mostly composed of medium sand, suggesting a high energetic deposition period (Photo 7). The bottom of the core is mostly organic rich (Photo 8).

## Sediment facies

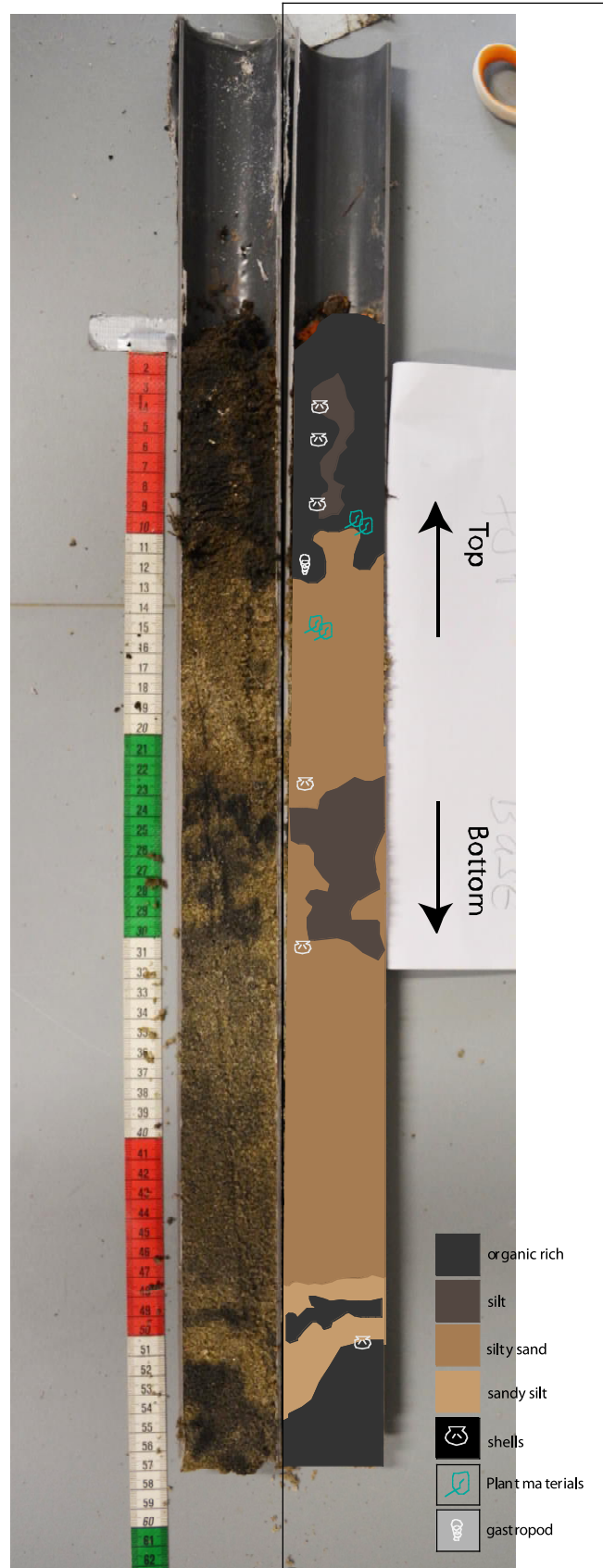


**Figure 3:** Sediment facies from sediment core C3.



**Photo 5:** Zoom to the top of the sediment core C3, showing the organic matter deposition.



**Photo 6:** Photo from the first half of core C3, showing the moisture of organic matter and sand.

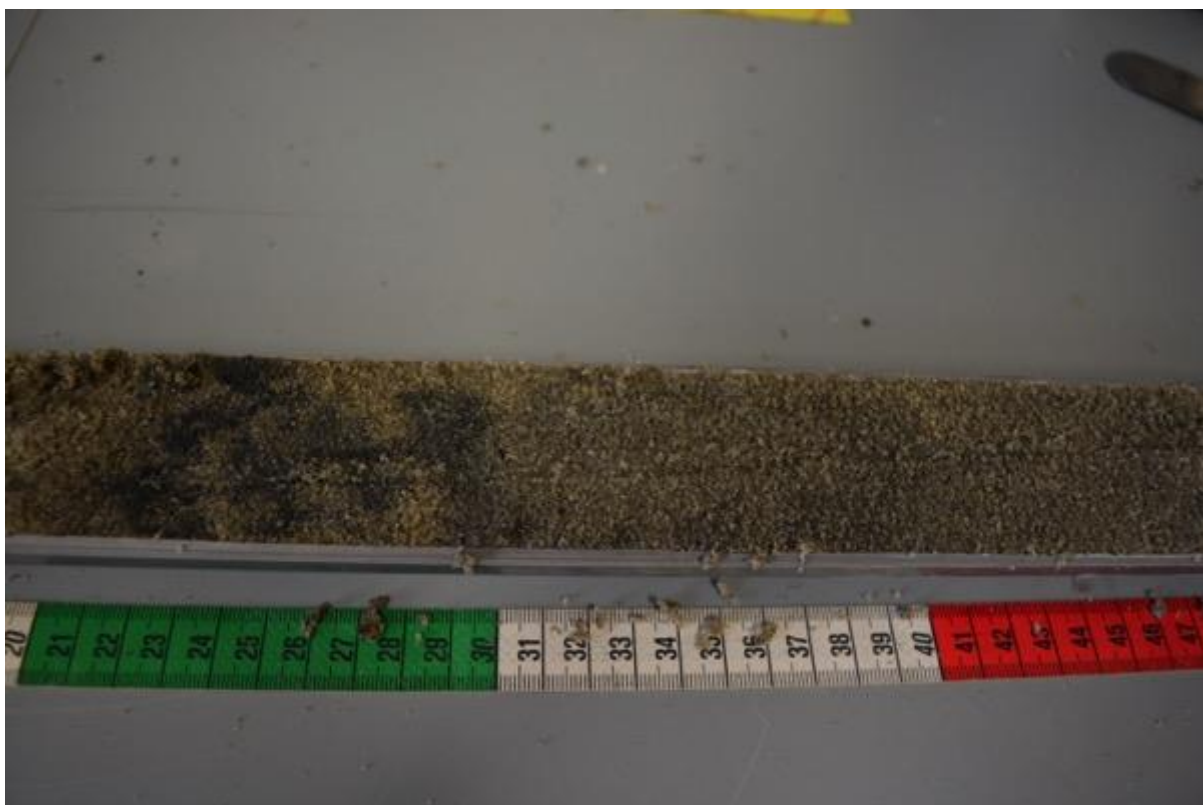


**Photo 7:** Photo from the second half of core C3, showing predominant medium sand.

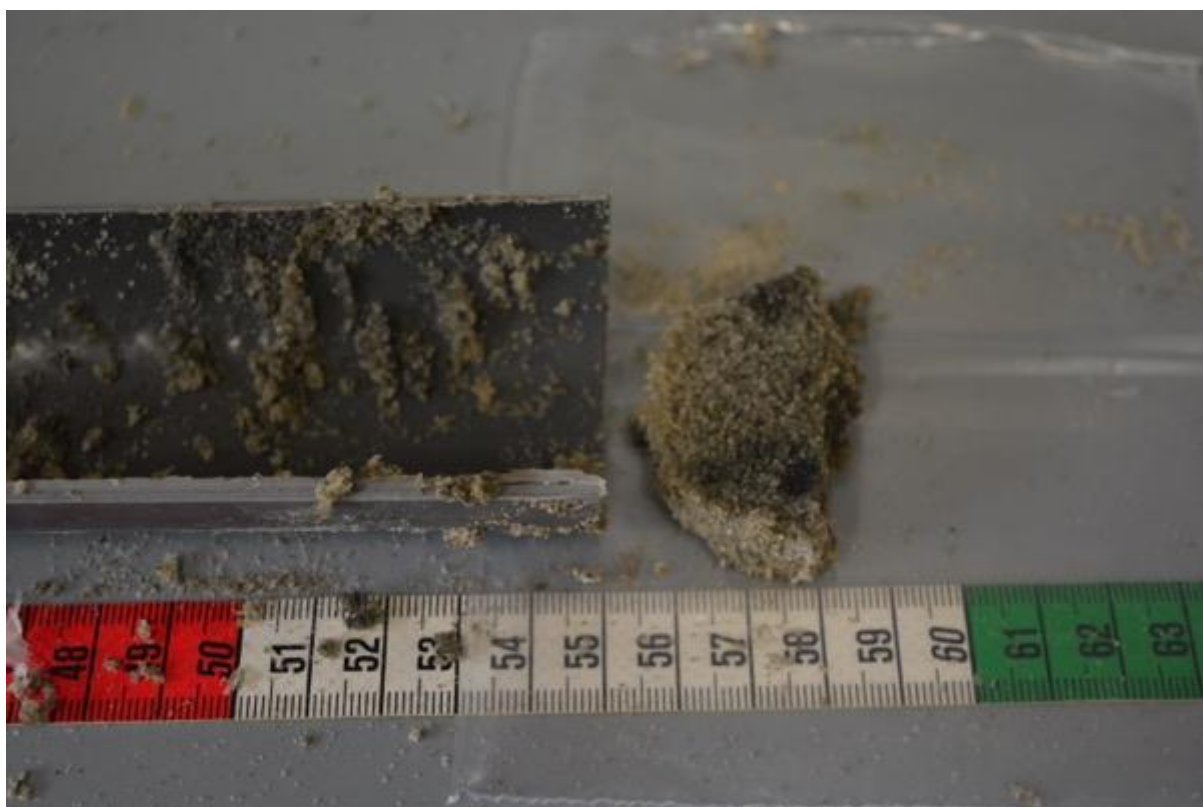


**Photo 8:** Zoom to the bottom of the sediment core C3 showing organic matter presence.

## 2 MEASUREMENT RESULTS

### 2.1 Profiling

An example of the profiles collected along three indicative tracks is given in Figures 4, 5 and 6, for Tracks 1, 2 and 3, respectively (the horizontal trajectories are given in figure 4).

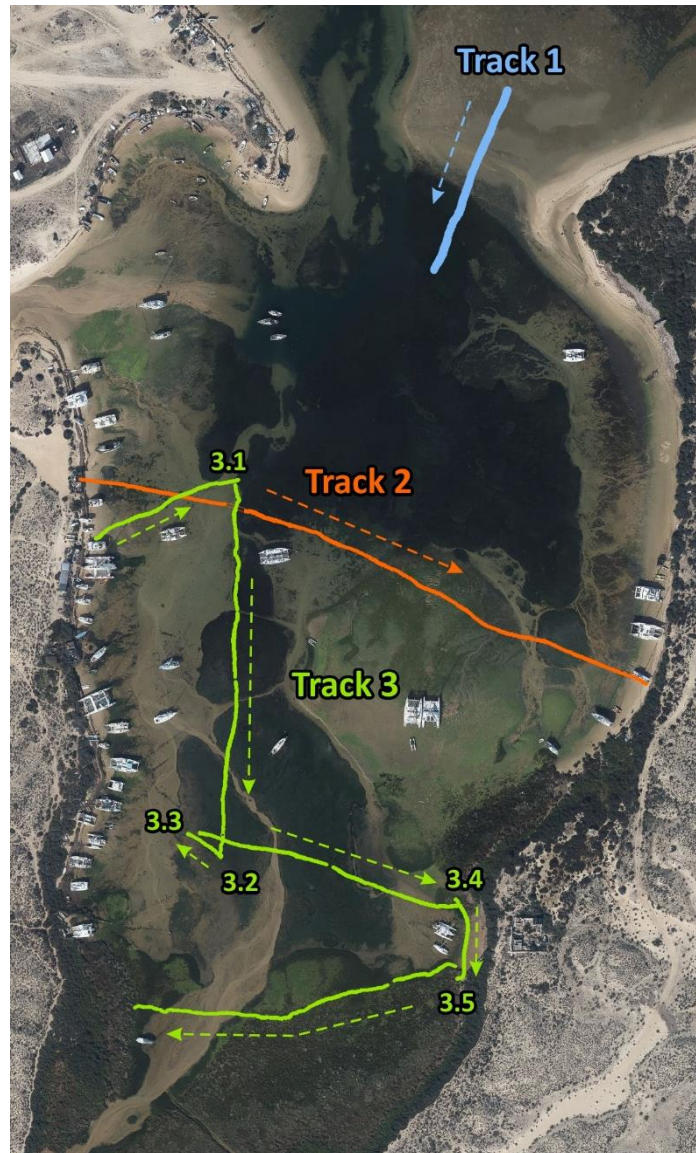


**Figure 4:** Trajectories of three tracks, whose measurements are indicatively presented. The direction of each track is presented as dashed arrow, while for Track 3, characteristic positions along the trajectory are given in as numbers 3.1 to 3.5.

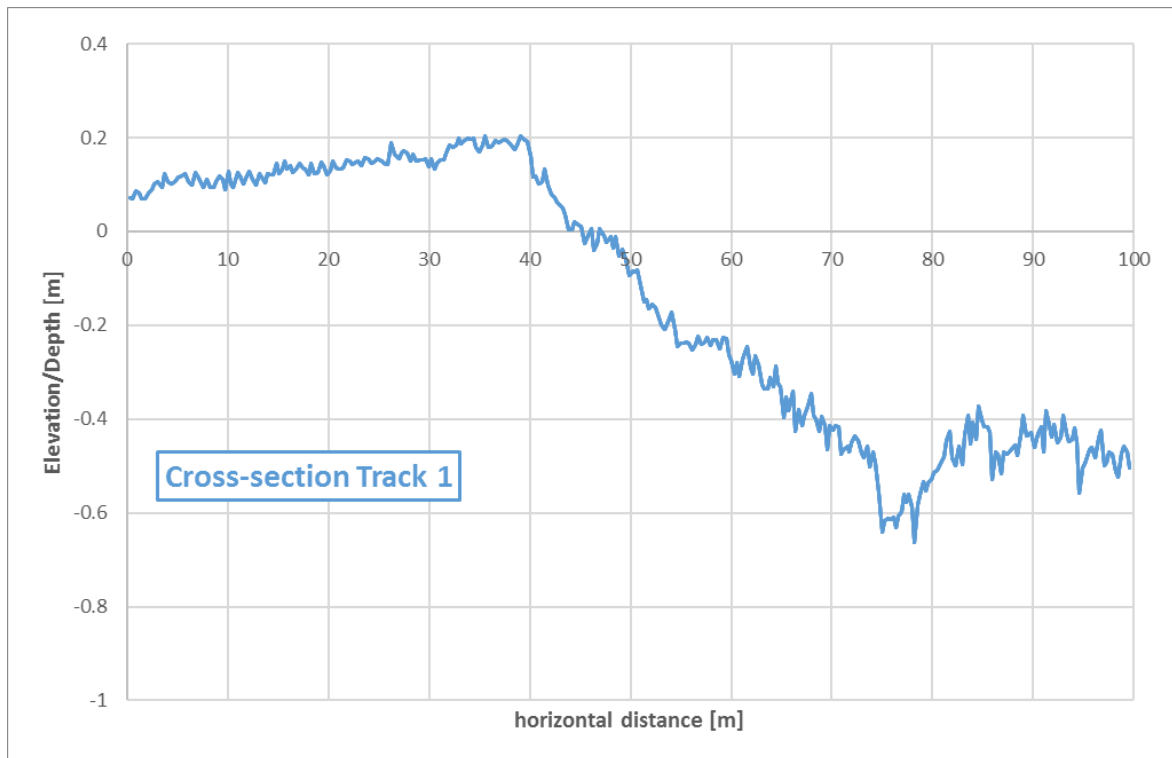


**Figure 5:** Profile along Track 1 (location of track is given in figure 4)

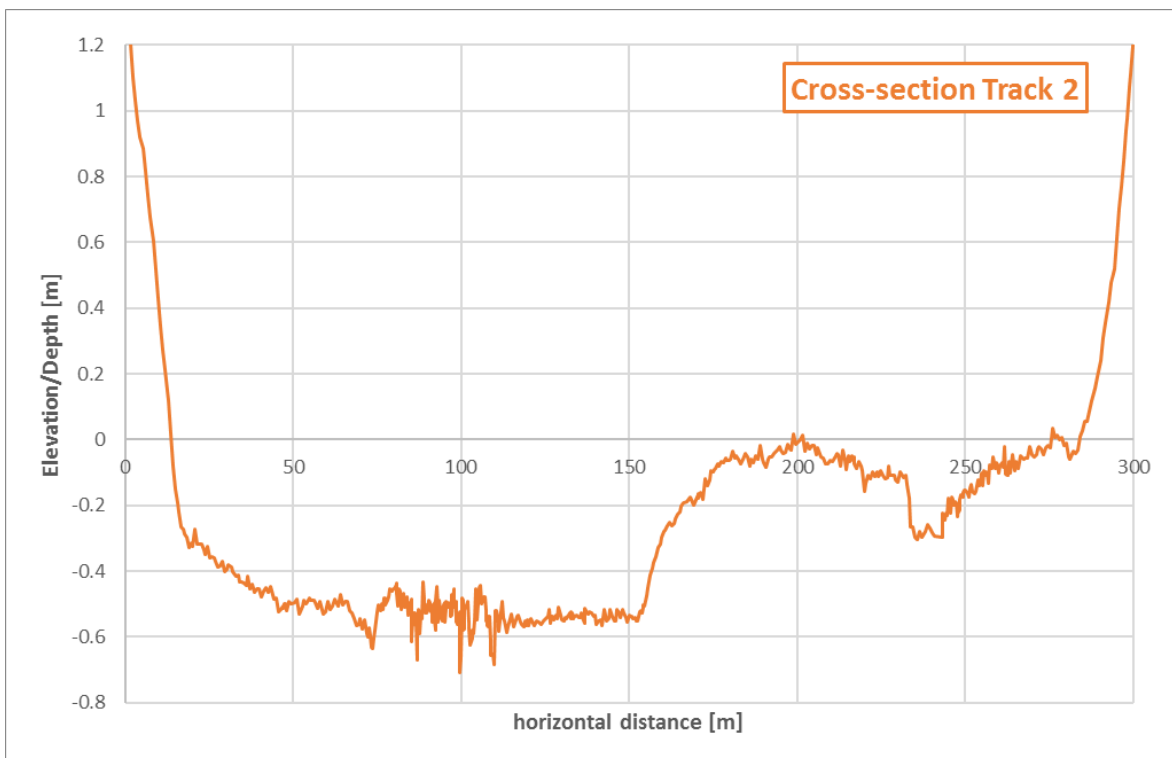


**Figure 6:** Profile along Track 2 (location of track is given in figure 4)

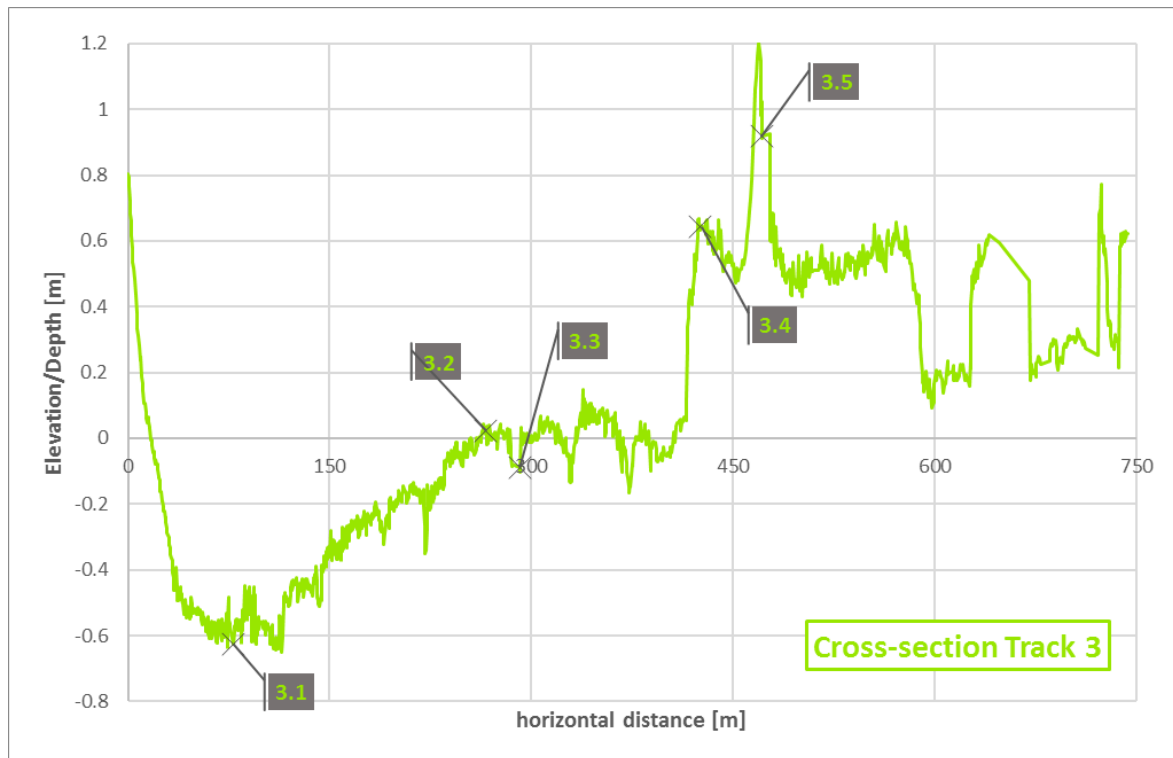


**Figure 7:** Profile along Track 3 (location of track is given in figure 4 and positions of change in track direction are noted as points 3.1 to 3.5).

## 2.2 Surface Sediment Properties

The 35 sediment samples collected were analysed in the laboratory in terms of granulometry and organic content. The samples were oven-dried and mechanically sieved, using sieves of 11200, 8000, 5600, 4000, 2800, 2000, 1400, 1000, 710, 500, 355, 250, 180, 125, 90 and 63 $\mu$ m. The material collected in each of the sieves was weighed, thus producing the granulometric distribution of coarse fraction, while the fine fraction, collected in the blind bottom pan, was analysed using laser granulometry.

The grain size distribution and statistics for all collected samples were defined using the GRADISTAT v.8.0 program (Blott & Pye, 2001). The program provides statistics regarding the sample distribution according to Folk and the method of moments, including mean diameter, sorting, skewness and kurtosis of the sample, while it also enables the automated production of graphs (cumulative and non-cumulative grain size distribution, gravel-sand-mud and sand-silt-clay diagrams after Folk).

The results of the sedimentological analysis are given in figure 8 for sand, mud and gravel and mean sediment diameter and in figure 9 for the percentage of organic content and for the sediment sorting type. It can be noted that the areas of high mud content (and, therefore, lower mean diameter) correspond to the vegetated areas of the bay (see more on vegetation in next section). As anticipated, there is high correlation between mud content and organic content in the sediment, while, at the same time, sediment sorting in these areas tends to be poor.

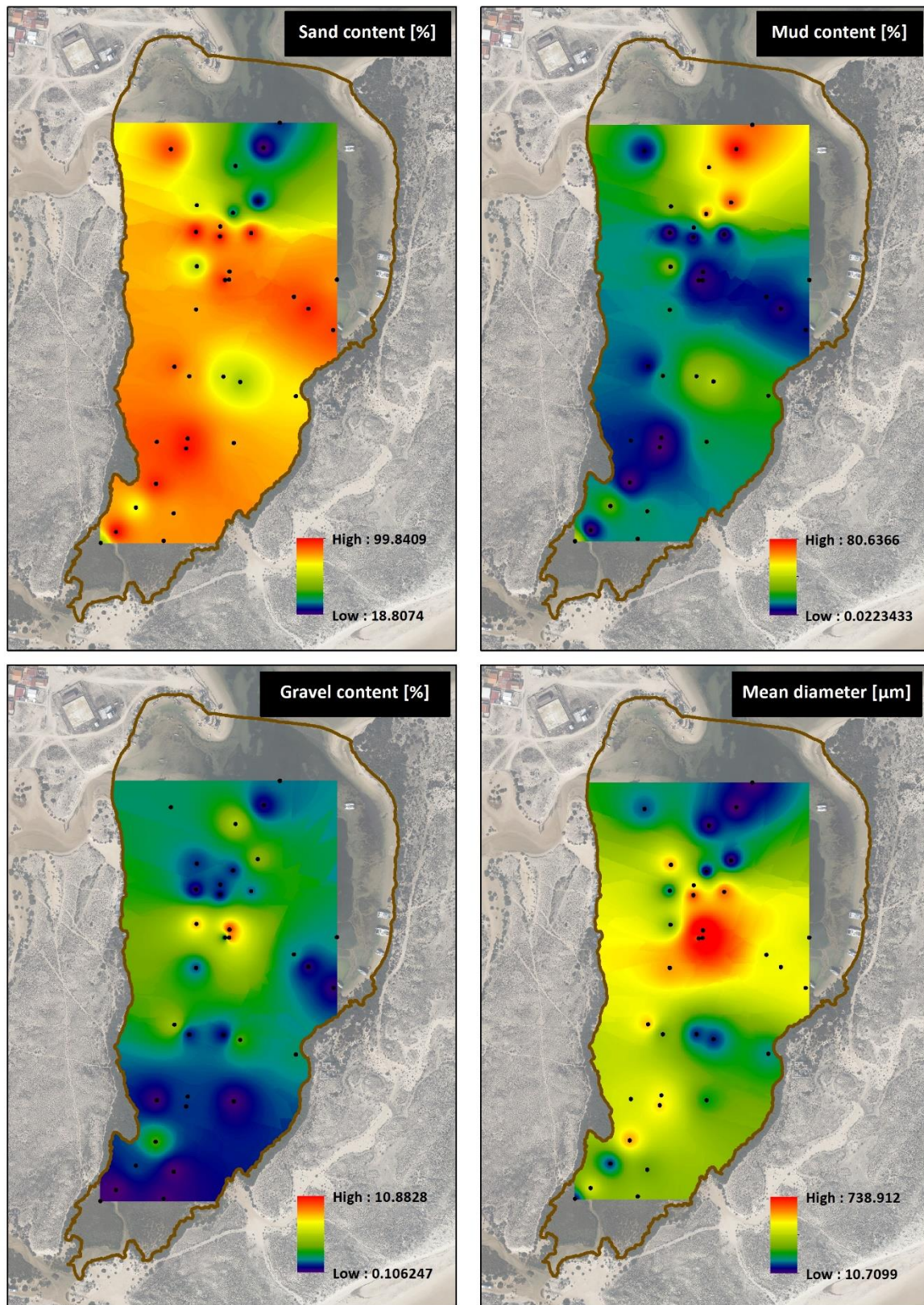


**Figure 8:** Distributions of sand, mud and gravel content and mean sediment diameter. The sampling stations' locations are noted with black dots.

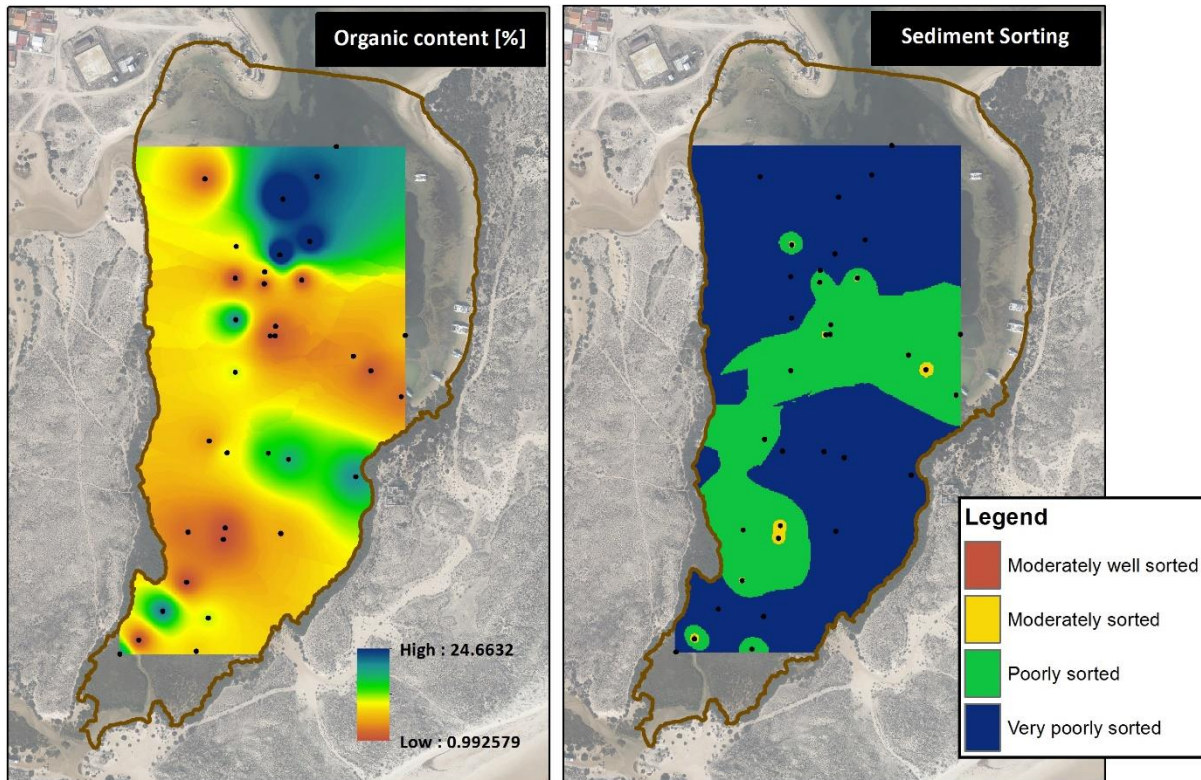


Figure 9: Organic content [%] and sediment sorting classification after Folk & Ward (1957).

## 2.3 Sediment Core analysis

### 2.3.1 Grain-size analysis of core C1

The results from the granulometric analysis of Core C1 (see Figure 2 for sampling location) are given in figure 10 regarding the depth distribution of gravel, sand and mud, the mean diameter (Folk & Ward, 1957) and the organic content of the sediment. The upper 5cm of the core contain sediment with a significant fine fraction (50%) and mean sediment diameter around  $20\mu\text{m}$ , characterised as coarse silt. The sand content increases with depth up to the layer of 9.5cm, with mean sediment diameter values of  $65\mu\text{m}$  to 0.35mm. Below 9.5cm, the sediment becomes more homogenous (sorting varies from moderately to moderately well), comprising medium sand ( $D_{50}=0.31\text{--}0.37\text{mm}$ ). The organic content in the core is relatively low and varies little with depth, ranging between 1.5 and 2.5%.

Figure 11 shows the relationship between organic content, mean sediment diameter and sediment sorting for core C1. Given that the organic content in the core varies little with depth, no direct conclusions can be drawn, even though the upper, finer upper 5 cm of the core do appear slightly richer in organic matter. The poor sorting of the surface sediment is related to the fine fraction in the mixture; this can be seen by the grain size distributions of the upper layers (Figure 12) show that the bimodality of the samples presents one peak at the clay size ( $2\mu\text{m}$ ) and another at fine to medium sand (0.25mm). This poor sorting of the near-surface layer could and the differences with the deeper parts of the core could signify different sediment sources and/or depositional patterns between the upper and the lower core.

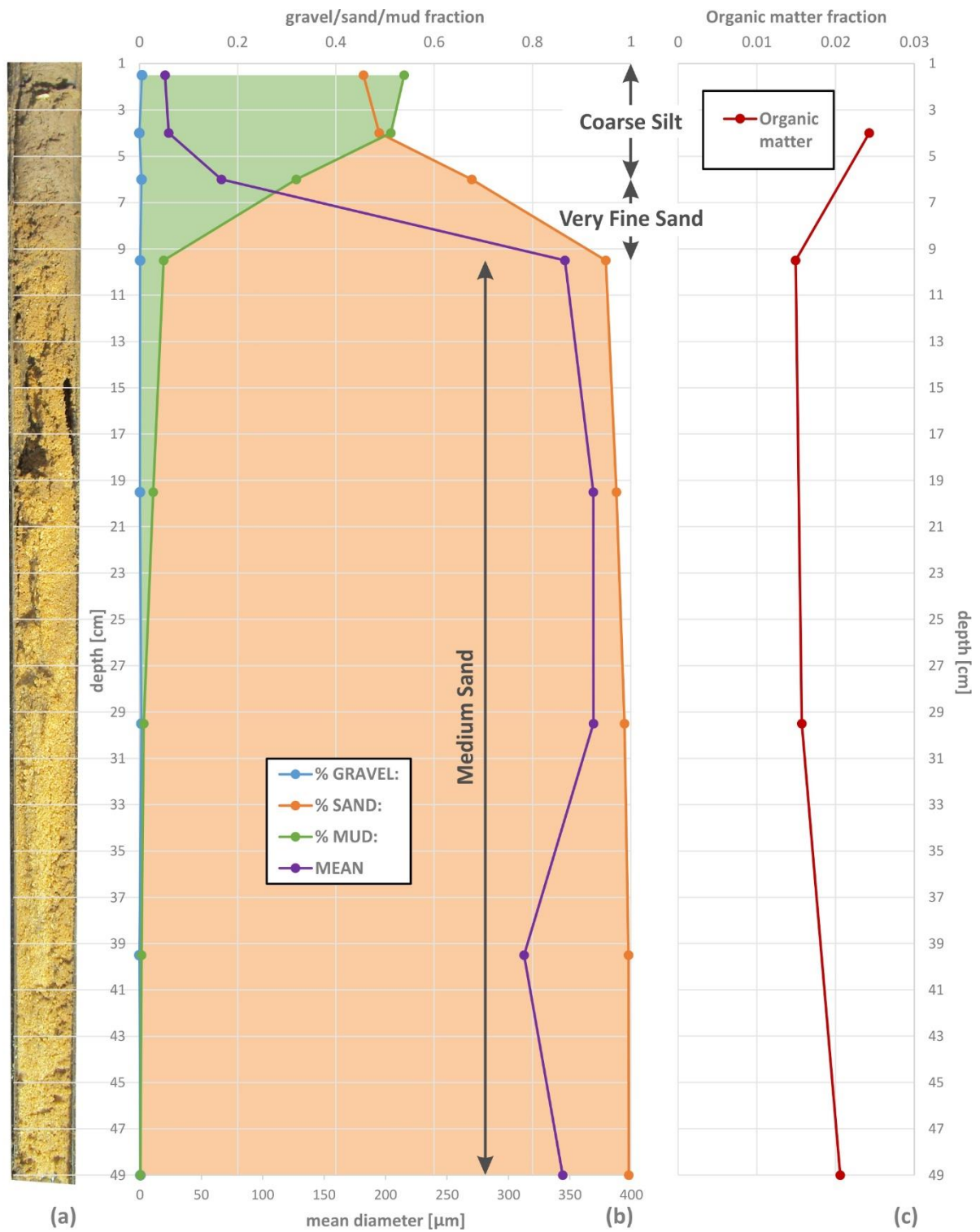


**Figure 10:** Distribution with depth of: (b) percent gravel, sand and mud (with reference to the top x-axis) and mean sediment diameter (with reference to the bottom x-axis) and (c) of organic content from the granulometric analysis of Core C1. A photo of the entire core, in scale with the plots, is given in (a), while the sediment description (according to Folk & Ward, 1957) is also noted on the graph.

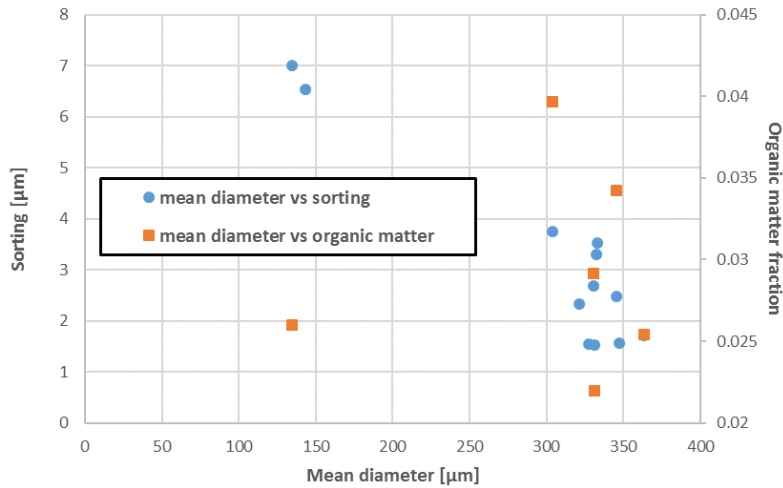


**Figure 11:** Variability of mean sediment diameter with sediment sorting (left y-axis) and organic matter (right y-axis) in the sediment of core C1.

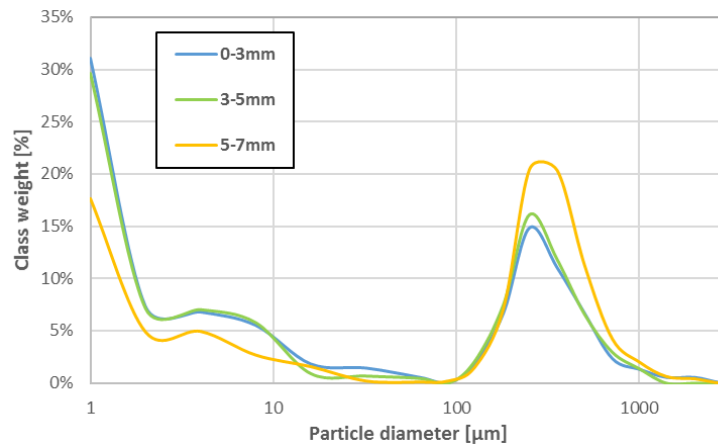


**Figure 12:** Particle size distribution for the upper three sediment layers of core C1.

### 2.3.2 Grain-size analysis of core C2

The results from the granulometric analysis of Core C2 (see Figure 2 for sampling location) are given in figure 13 regarding the depth distribution of gravel, sand and mud, the mean diameter (Folk & Ward, 1957) and the organic content of the sediment. There is a local peak in fine fraction content in the layer between 7 and 11cm that is accompanied by a reduction in sand content and diameter ( $D_{50}=0.14\text{mm}$ , fine sand). In the top 7cm and the layers below 15cm the sediment is characterised as medium sand, with mean sediment diameters of 0.3-0.36mm. The organic content in the core is relatively low and varies little with depth, ranging between 2 and 4%. The distribution of sediment with depth in the top part of core C2 (top 7cm) is atypical and very different from the ones in cores C1 and C3 (see next section), where the peak in mud content appears in the surface. The high sand content in the top layer is most likely related to the proximity of the location to the sandy channel in relation with the local hydrodynamics.

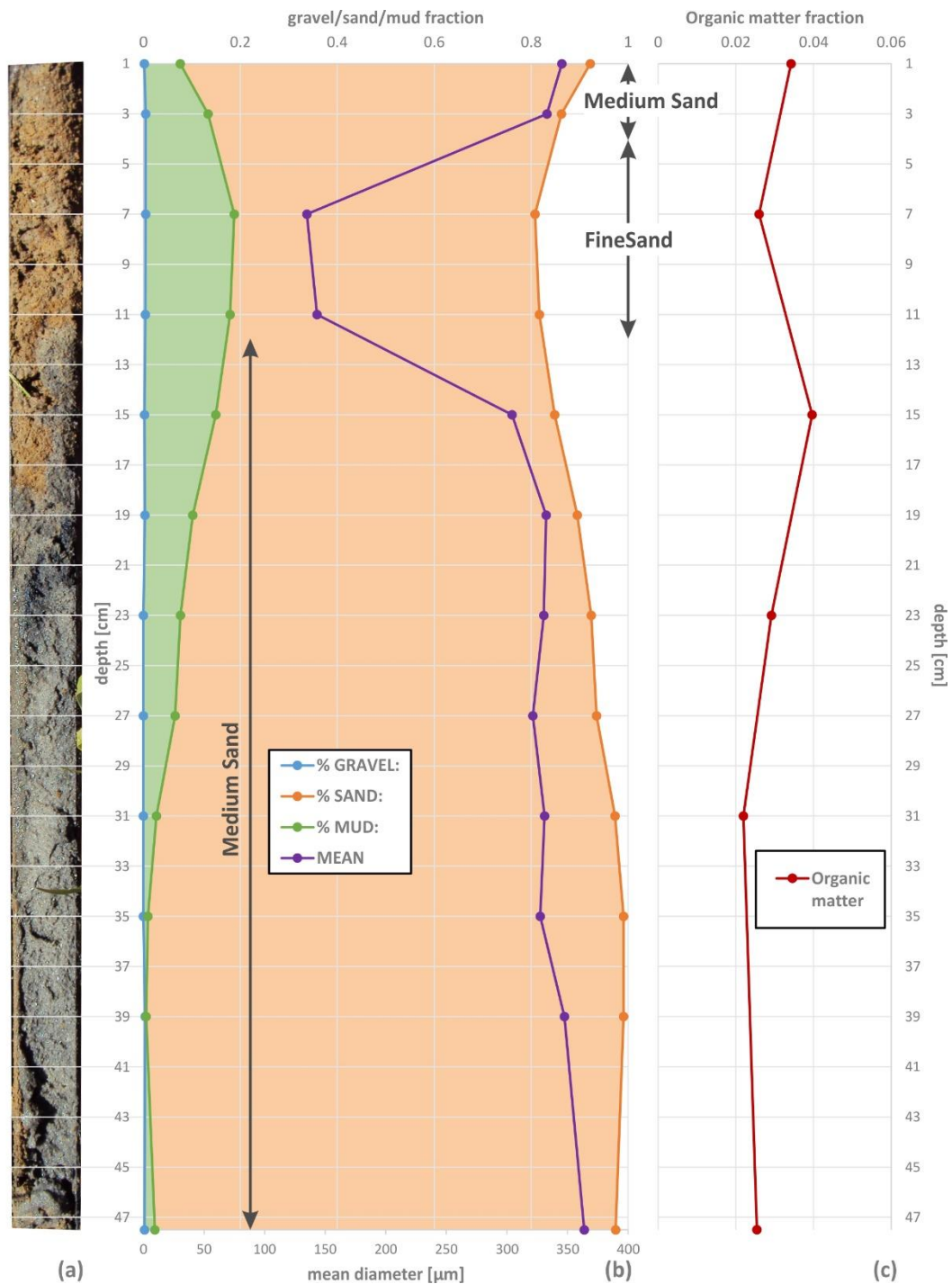


**Figure 13:** Distribution with depth of: (b) percent gravel, sand and mud (with reference to the top x-axis) and mean sediment diameter (with reference to the bottom x-axis) and (c) of organic content from the granulometric analysis of Core C2. A photo of the entire core, in scale with the plots, is given in (a), while the sediment description (according to Folk & Ward, 1957) is also noted on the graph.

Figure 14 shows the relationship between organic content, mean sediment diameter and sediment sorting for core C2. Given that the organic content in the core varies little with depth, no direct conclusions can be drawn, while the sorting appears to be strongly related to the mean diameter. Figure 15 presents the grain size distributions of the upper layers of the core. s

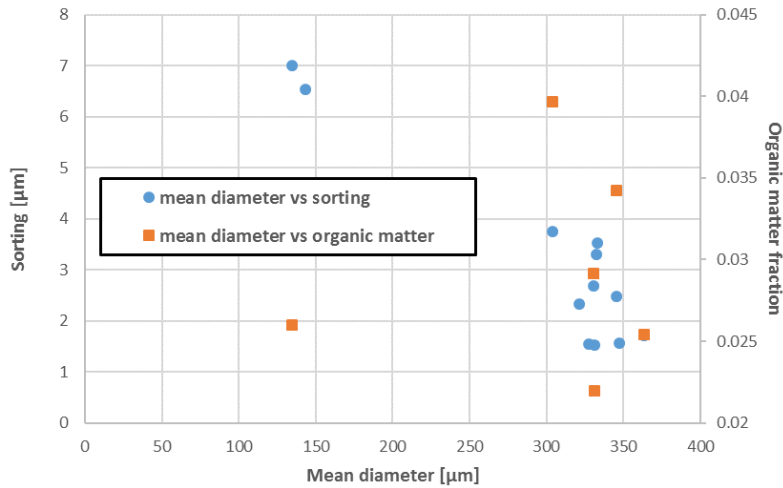


**Figure 14:** Variability of mean sediment diameter with sediment sorting (left y-axis) and organic matter (right y-axis) of core C2.

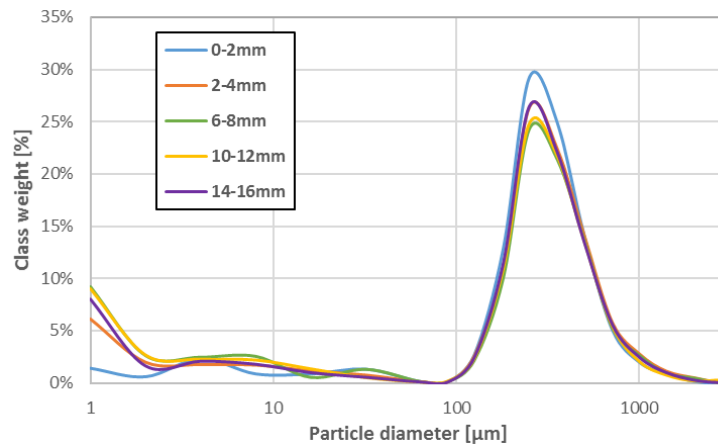


**Figure 15:** Particle size distribution for the upper five sediment layers of core C2.

### 2.3.3 Grain-size analysis of core C3

The results from the granulometric analysis of Core C3 (see Figure 2 for sampling location) are given in figure 16 regarding the depth distribution of gravel, sand and mud, the mean diameter (Folk & Ward, 1957) and the organic content of the sediment. The upper 12cm of the core are organic-rich layers with significant fine fraction (>20%), mean sediment diameter between 60 and 140μm and poor sorting. Below 12cm, the sediment becomes more homogenous (sorting varies from moderately to moderately well), comprising medium sand ( $D_{50}=0.35-0.40\text{mm}$ ) and with low organic content (<4%). The coarser sediment (gravel) observed in the upper core are shell fragments (Figure 3).

Similar conclusions can be drawn from figure 17 that shows the relationship between organic content, mean sediment diameter and sediment sorting. It can be noted that the deeper, coarser layers of the core are rather well sorted and, as noted before, contain less organics, while the opposite is true for the upper. The poor sorting of the surface sediment is related to the fine fraction in the mixture; this can be seen by the grain size distributions of the upper layers (Figure 18) show that the bimodality of the samples presents one peak at the clay size (2μm) and another at fine to medium sand (0.25mm). This bimodal structure of the near-surface layer could signify different sediment sources and/or depositional patterns between the upper and the lower core.

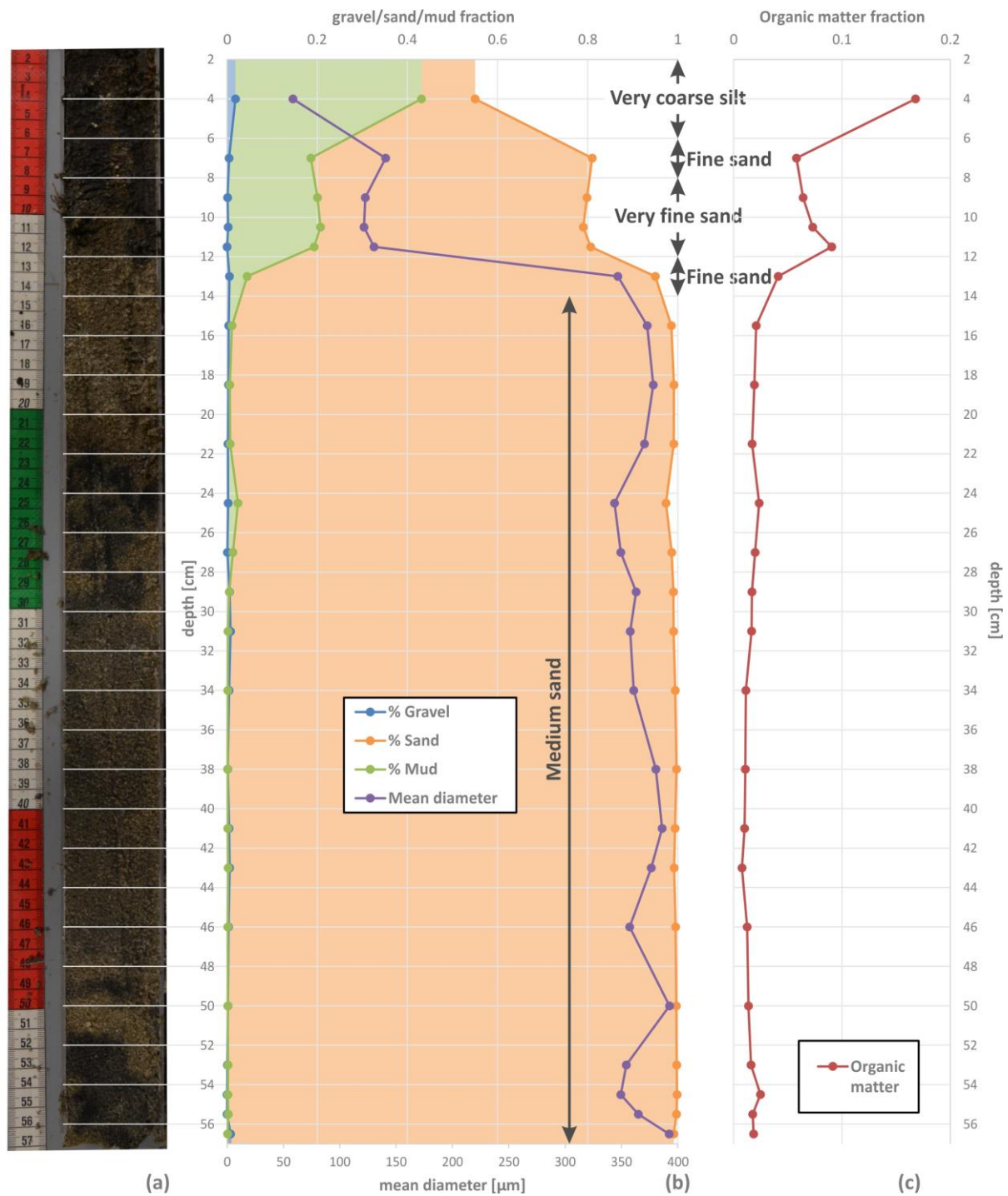


**Figure 16:** Distribution with depth of: (b) percent gravel, sand and mud (with reference to the top x-axis) and mean sediment diameter (with reference to the bottom x-axis) and (c) of organic content from the granulometric analysis of Core C3. A photo of the entire core, in scale with the plots, is given in (a), while the sediment description (according to Folk & Ward, 1957) is also noted on the graph.

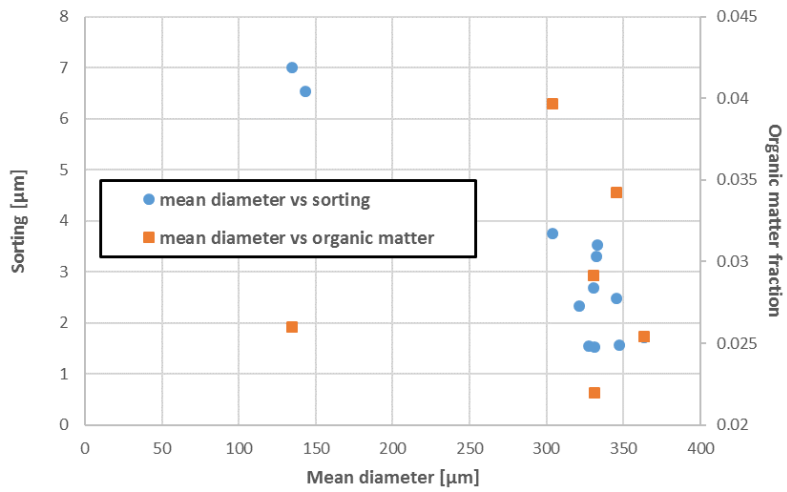


**Figure 17:** Variability of mean sediment diameter with sediment sorting (left y-axis) and organic matter (right y-axis) of core C3.

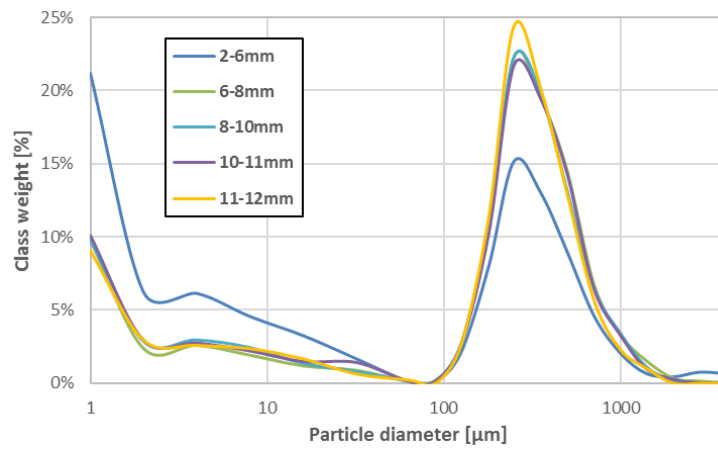


**Figure 18:** Particle size distribution for the upper five sediment layers of core C3.

### 3. IDENTIFICATION OF INTERTIDAL AND MARSH VEGETATION

In the following images (Photo 9 to Photo 13), photographic records are given for the sediment sampling stations (2 for each station). For the exact locations of the stations and their distribution in the bay, the reader is directed to figure 1 and table 1. Photo 17 shows a panoramic view of the entire Bay, with a more general view of the morphology and intertidal vegetation distribution and coverage in the area. It can be noted from the photos that the dominant species in the muddy areas of the tidal flat and low marsh is *Zostera noltei* with dense meadows in stations 1, 2, 9, 16 and lower population densities in stations 14 and 15. The deeper channels and low-depth plateau in the central part of the bay consist of sandy matter with no rooted vegetation (stations 4, 5, 6, 7, 8, 20 & 22), while floating vegetation (*Ulva*) was also present in areas of the plateau (station 6). The upper part of the marsh in the southern part of the bay is muddy (stations 3, 19 & 21) and vegetated with a succession of *Spartina maritima* (Photo 14), *Salicornia ramosissima* (Photo 15) and *Limoniastrum monopetalum* (Photo 16). The succession can also be seen in photo 18. The edge of the *Limoniastrum monopetalum* presence in the upper marsh defines a distinct 'barrier' in the domain, which was mapped during the field campaign and is presented as purple line in figure 2. Other species, such as *Sarcocornia perennis*, *Arthrocnemum macrostachyum* and *Limonium ovalifolium*, were also present in the upper marsh, even though at lower densities compared to the three main species, mentioned previously. Dense meadows of *Zostera maritima* are found in stations 22 to 24 and cover the deeper parts of the bay, near the entrance; the specie is also found at the edges of *zostera noltei* meadows, developing along the sandy channels of the bay (Photo 19).

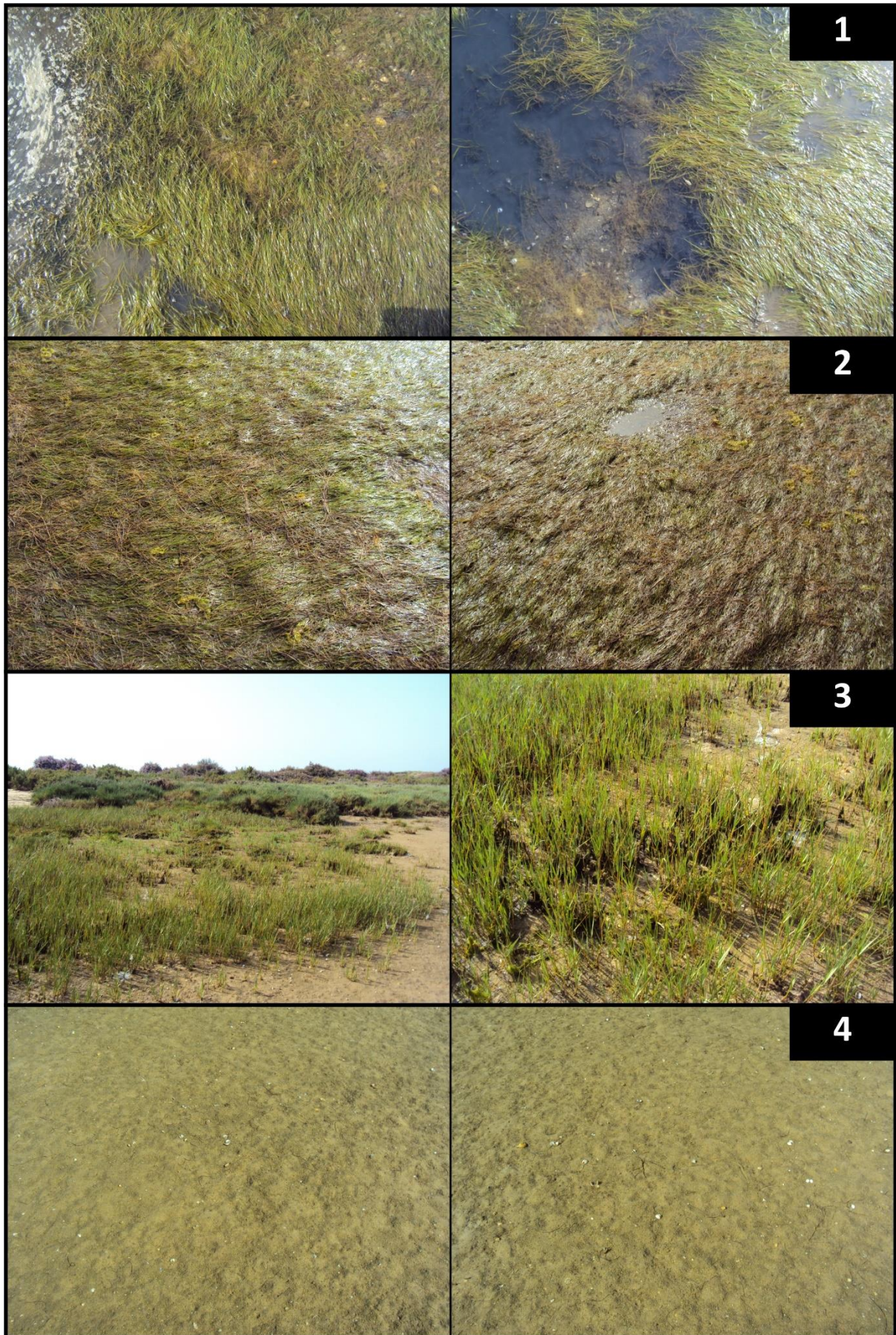


**Photo 9:** Photos from stations 1, 2, 3 and 4

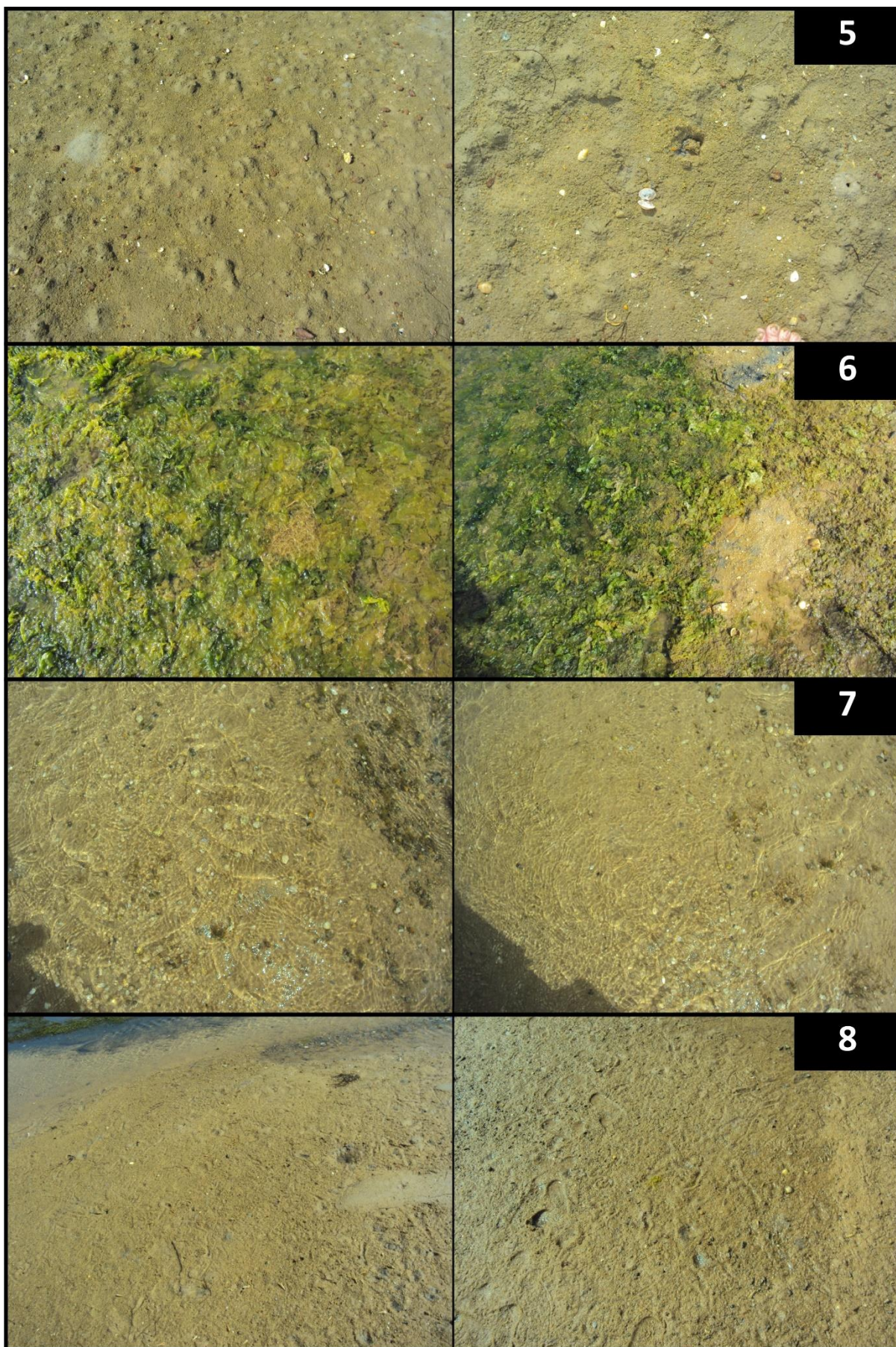


**Photo 10:** Photos from stations 5, 6, 7 and 8

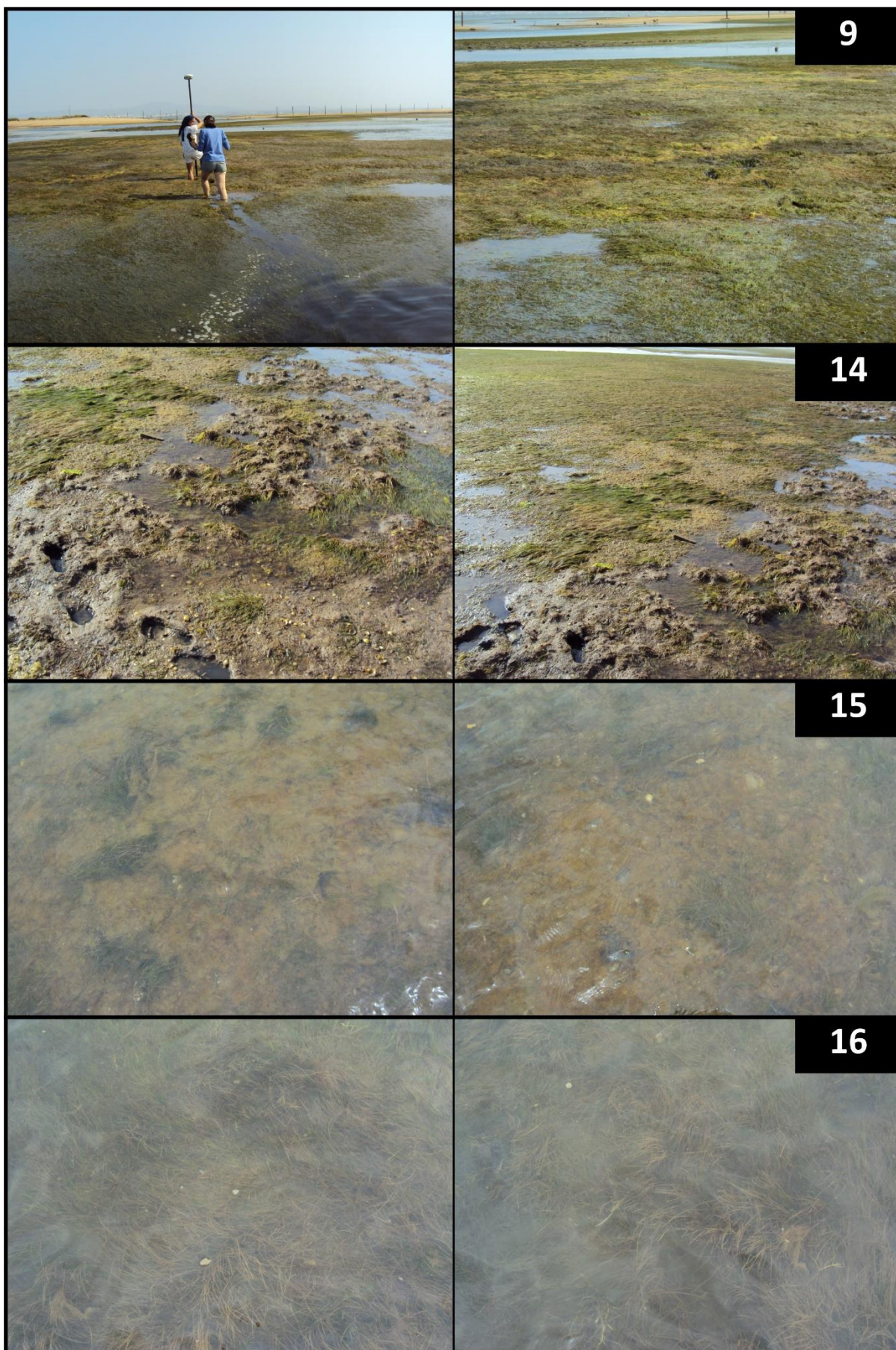


**Photo 11:** Photos from stations 9, 14, 15 and 16

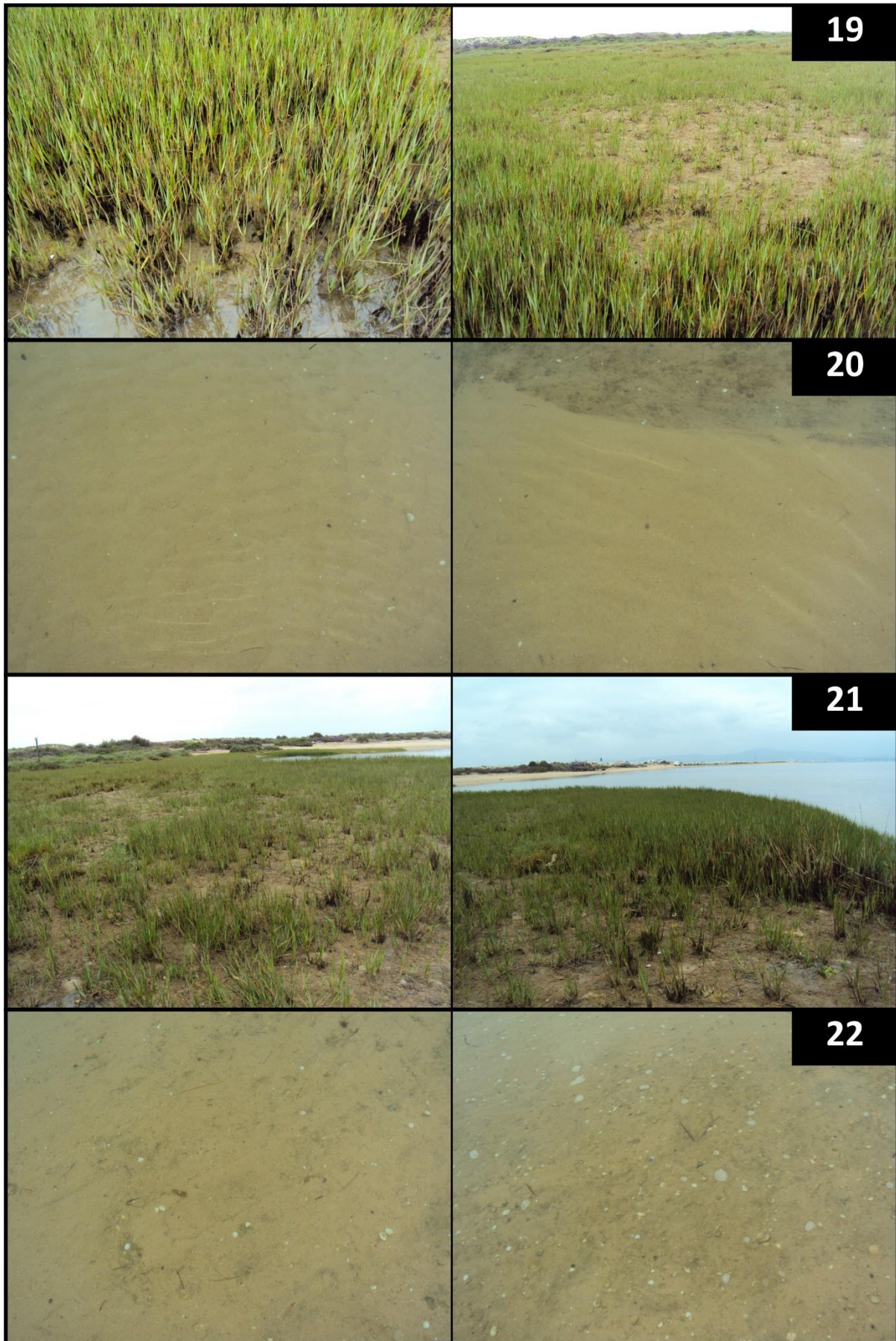


**Photo 12:** Photos from stations 19, 20, 21 and 22

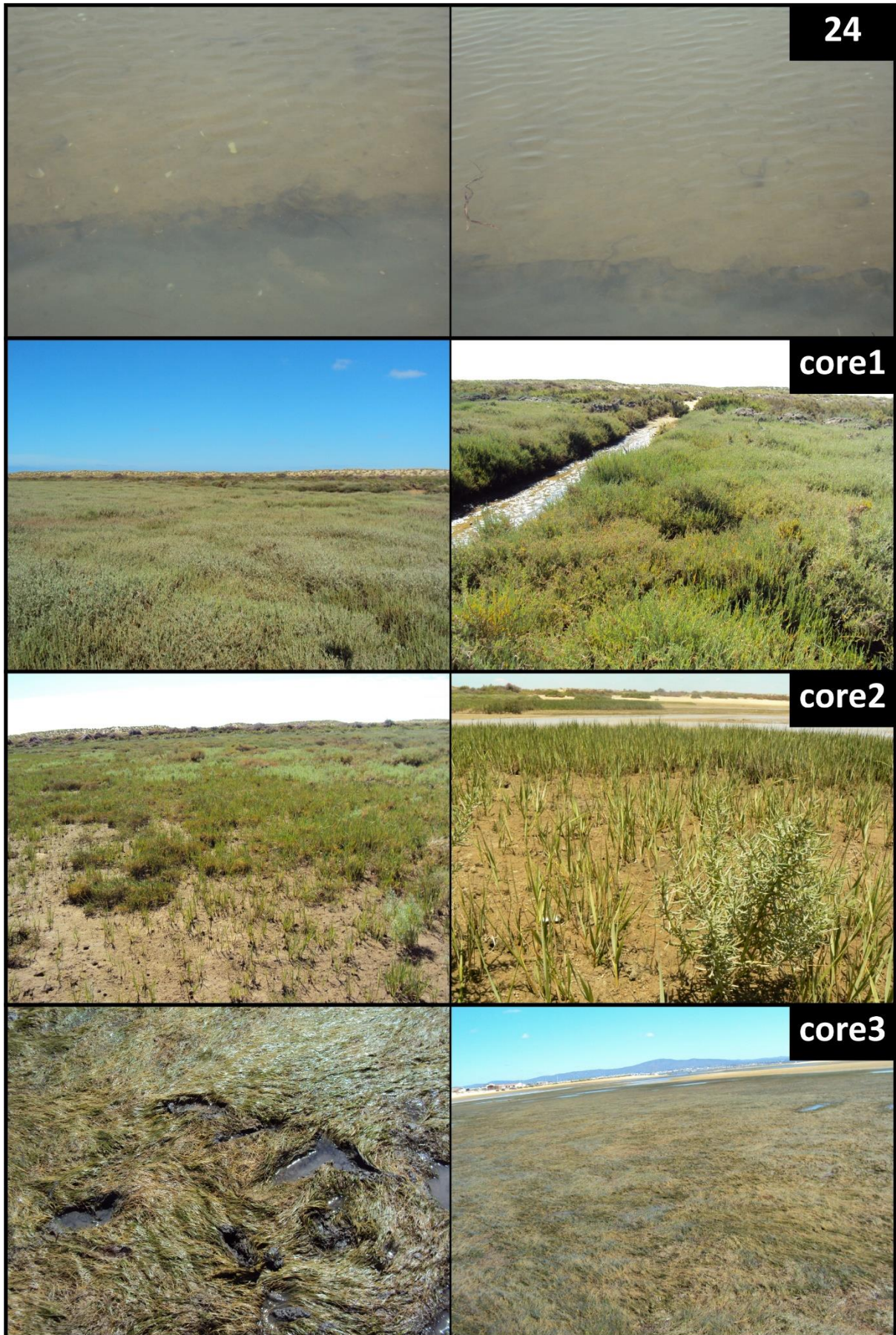


**Photo 13:** Photos from station 24 and cores 1, 2 and 3



**Photo 14:** *Spartina maritima* meadows, found at the low-upper part of the marsh (southern bay)



**Photo 15:** *Salicornia ramosissima*, found in the mid-upper part of the marsh (southern bay)

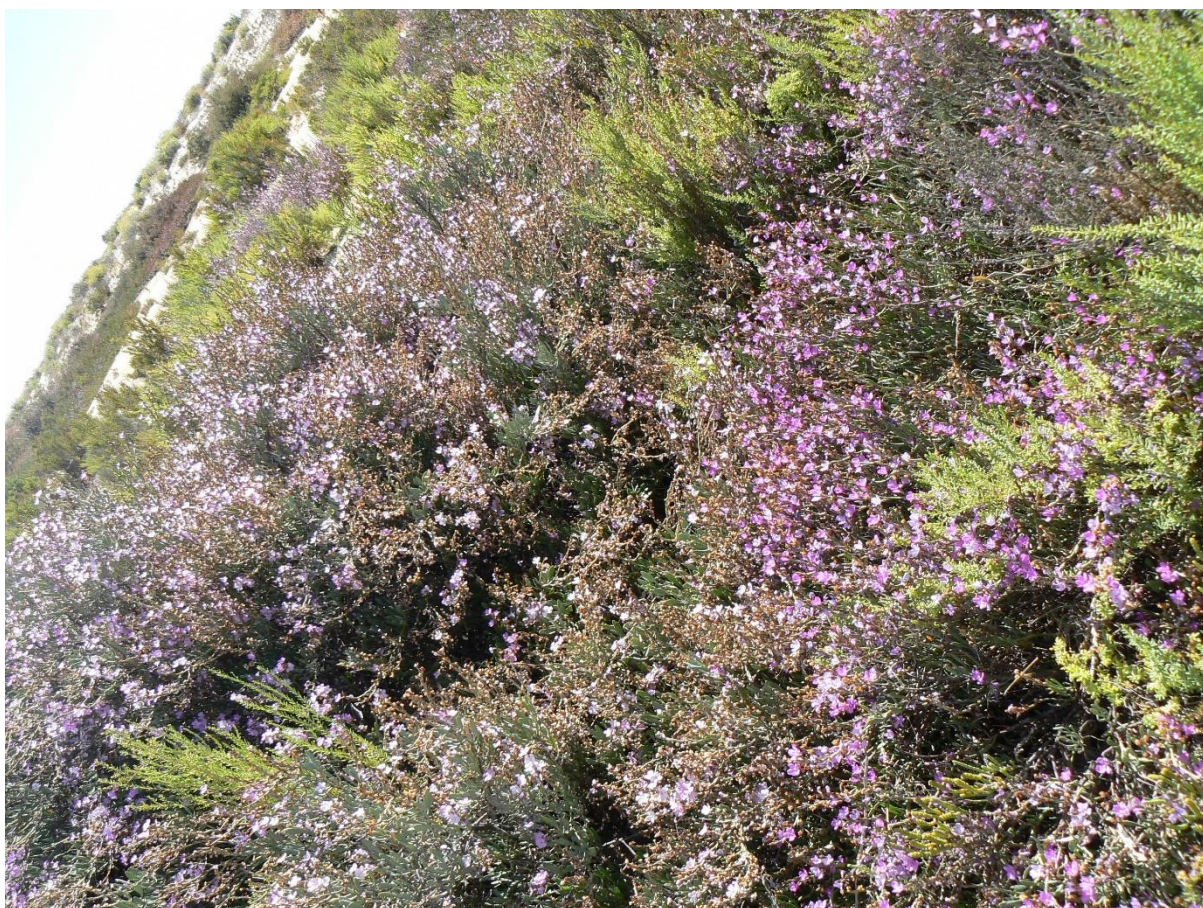


**Photo 16:** *Limoniastrum monopetalum*, found at the high-upper part of the marsh (southern bay)

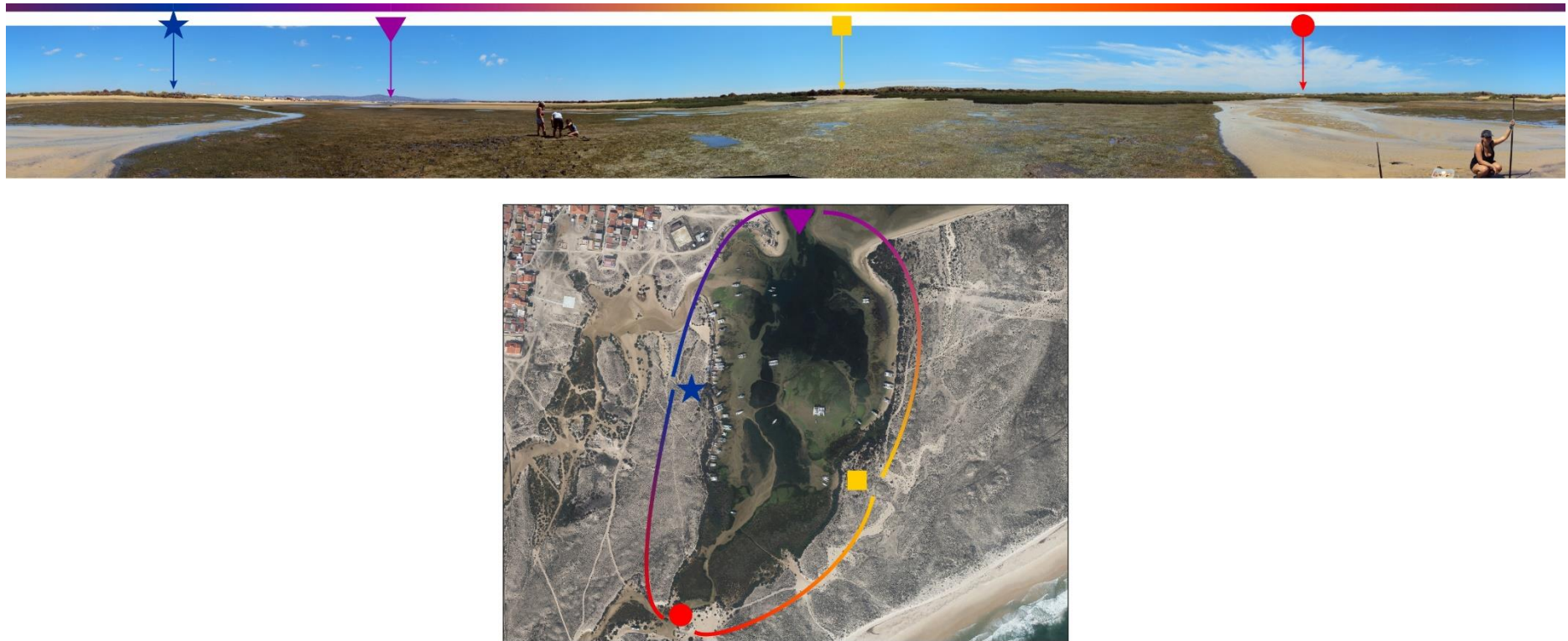


**Photo 17:** Panorama of the entire study area (top), produced after stitching series of photographs taken from approximately the middle of the bay. Four characteristic points are noted in the panoramic view of the area and are related to a vertical photo of the bay (bottom), along with colour-gradated curves that denote the transition between points, to facilitate orientation.

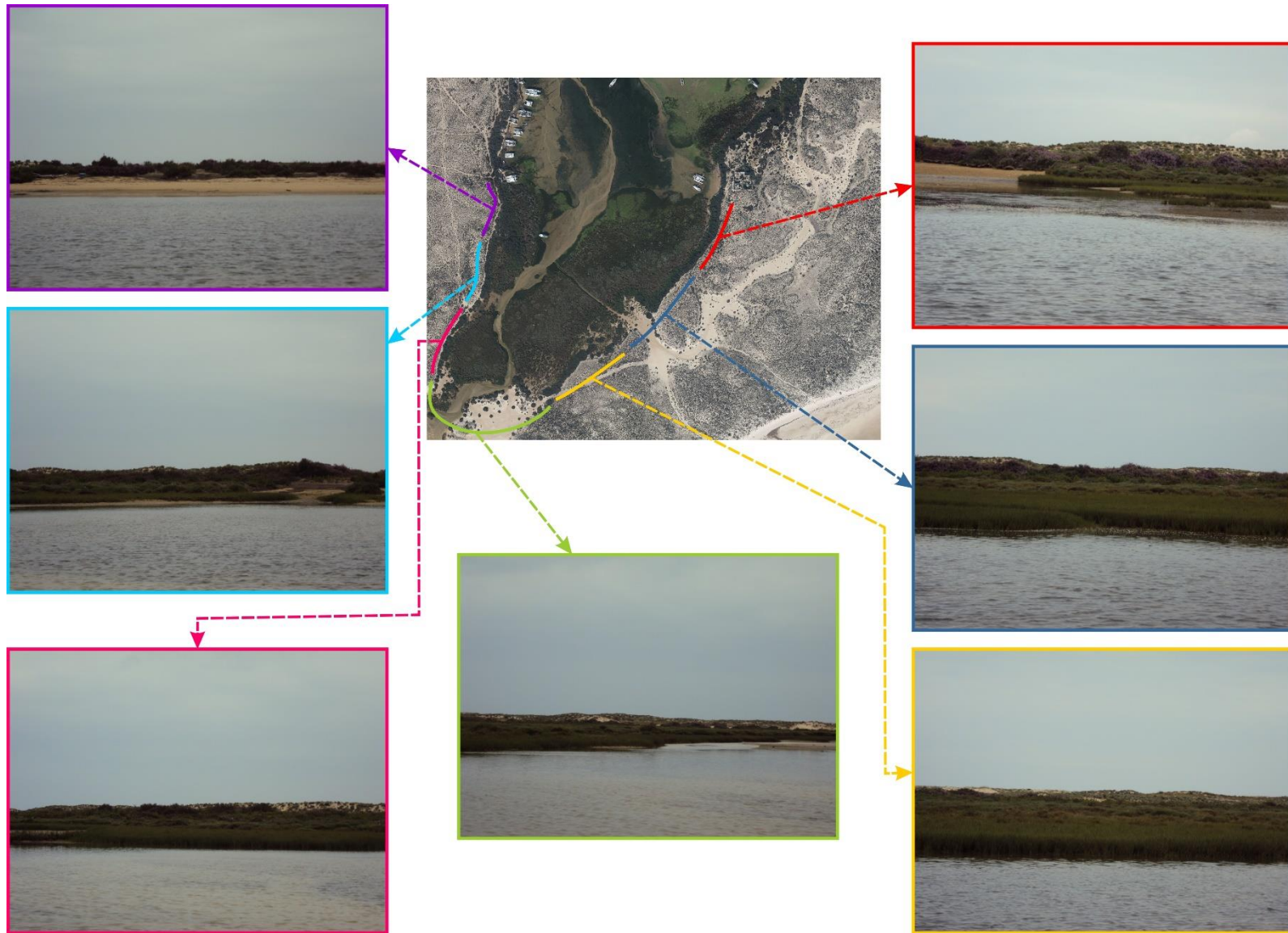


**Photo 18:** Series of 'panoramic' photos for the southern part of the bay, where the vegetation species succession in the upper marsh can be noted.

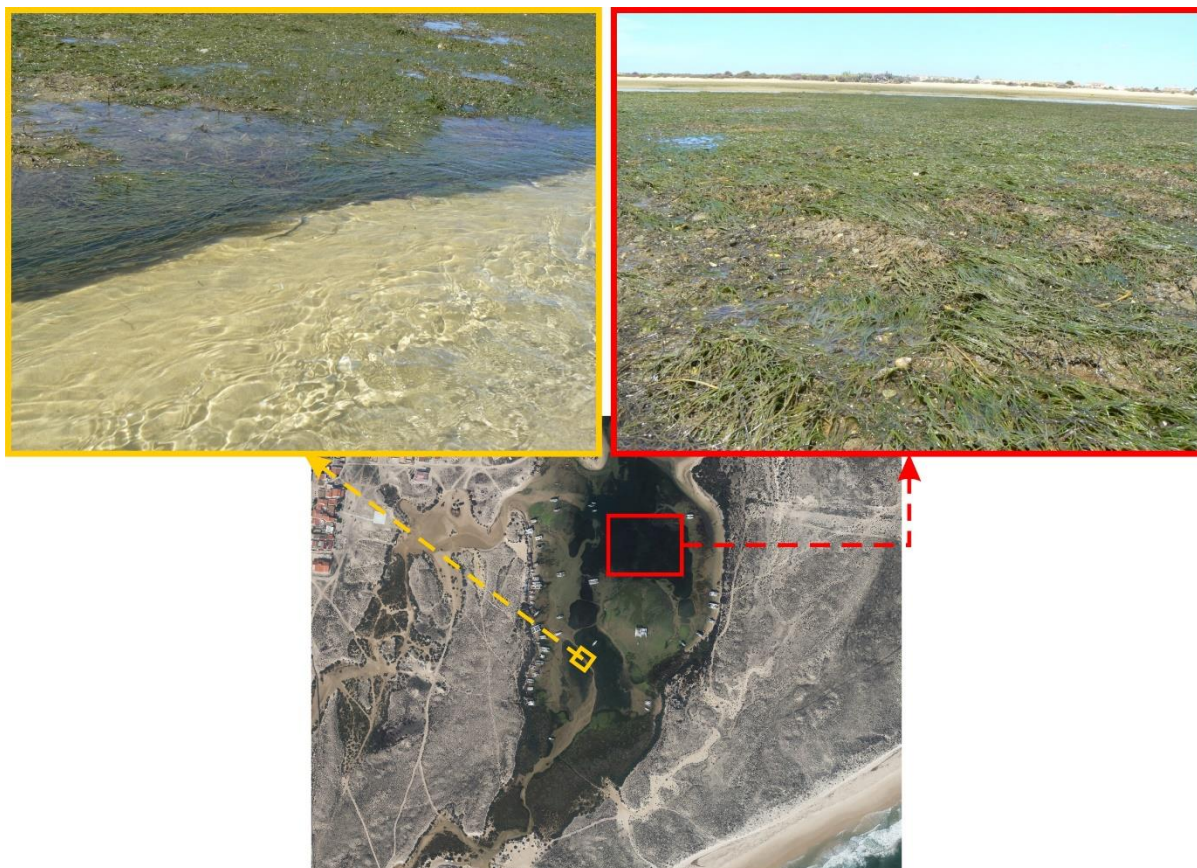


**Photo 19:** Presence of *zosteria marina* in the study area: a) at the edges of *zosteria noltei* meadows and along the sandy channels (yellow box) and b) development of dense *zosteria marina* meadows in the deeper parts of the northern bay (red box).

## REFERENCES

- Blott, S. J., & Pye, K. (2001). GRADISTAT: A GRAIN SIZE DISTRIBUTION AND STATISTICS PACKAGE FOR THE ANALYSIS OF UNCONSOLIDATED SEDIMENTS. *Earth Surface Processes and Landforms Earth Surf. Process. Landforms*, 26, 1237–1248. <https://doi.org/10.1002/esp.261>
- Folk, R. L., & Ward, W. C. (1957). Brazos River bar [Texas]; a study in the significance of grain size parameters. *Journal of Sedimentary Research*, 27(1), 3–26. <https://doi.org/10.1306/74D70646-2B21-11D7-8648000102C1865D>